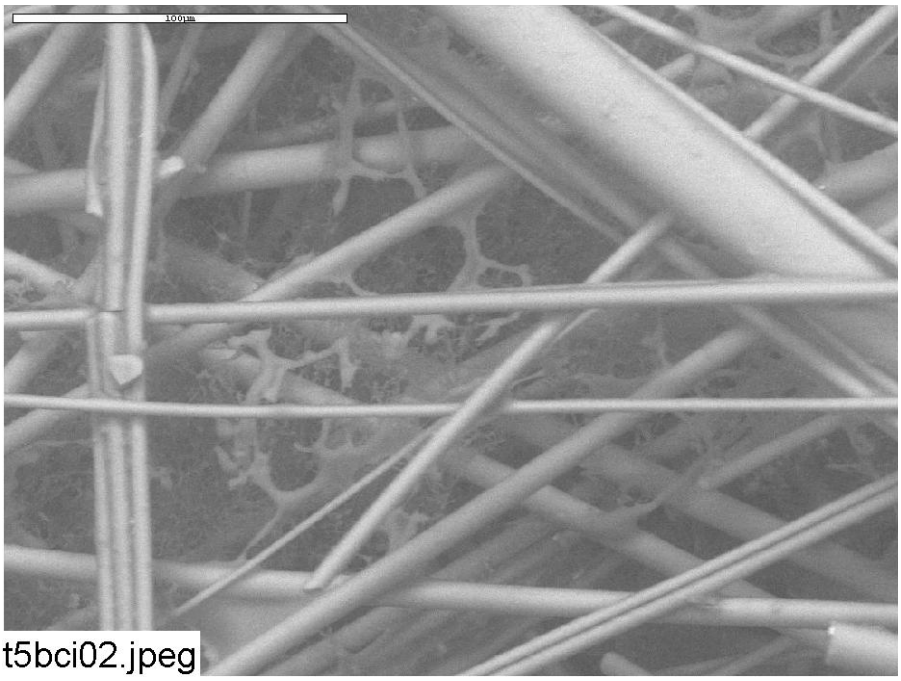

Figure 3-70. ESEM image magnified 500 times for a Test #5, Day-30 interior fiberglass sample in the birdcage.

3.4. Metallic and Concrete Coupons

3.4.1. Weights and Visual Descriptions

3.4.1.1. Submerged Coupons

Examination of the 40 submerged coupons provides insights into the nature of the chemical kinetics that occurred during this 30-day test. The physical change that these coupons experienced is determined through both visual evidence and weight measurement of each coupon before and after the test. Pre-test pictures were taken of the coupons when they were received and before they were inserted into the racks. Post-test pictures were taken several days after the racks had been removed from the tank. All racks with coupons still inserted were staged to allow the coupons to dry completely before the post-test pictures were taken. The coupons were placed in a low-humidity room and allowed to air dry. All coupons were also weighed before they were inserted into the tank and after the 30-day test was completed.

There are three submerged aluminum coupons in each test. Figures 3-71 through 3-73 are the pre- and post-test pictures of the Test #5 coupons. The aluminum coupons A1-240, A1-241, and A1-242 (see Figures 3-71 through 3-73) were located from east to west, respectively, in the tank. The submerged aluminum coupons turned brown, and they developed a brown, powdery film on the surface. The film resulted in the surface of the coupon becoming rough to the touch.

Figure 3-71. Al-240 submerged, pre-test (left) and post-test (right).

Figure 3-72. Al-241 submerged, pre-test (left) and post-test (right).

Figure 3-73. Al-242 submerged, pre-test (left) and post-test (right).

Figures 3-74 through 3-76 present the pre- and post-test pictures of three submerged galvanized steel coupons. The galvanized steel coupons developed a white precipitate on the surface of the coupons, which caused the surfaces to have a coarse feel. The surfaces of the coupons had horizontal lines composed of this same white precipitate. The horizontal deposits may have been left during the slow draining of the tank solution.

Figure 3-74. GS-137 submerged, pre-test (left) and post-test (right).

Figure 3-75. GS-140 submerged, pre-test (left) and post-test (right).

Figure 3-76. GS-141 submerged, pre-test (left) and post-test (right).

Figures 3-77 and 3-78 present the pre- and post-test pictures of two submerged IOZ-coated steel coupons. Both submerged IOZ-coated steel coupons have similar light particulate deposits. These coupons were covered with a brown coating over their entire surfaces.

Figure 3-77. IOZ-310 submerged, pre-test (left) and post-test (right).

Figure 3-78. IOZ-312 submerged, pre-test (left) and post-test (right).

Figures 3-79 and 3-80 present the pre- and post-test pictures of two submerged copper coupons. The submerged copper coupons developed very light horizontal white deposits, which may be due to the slow tank draining process.

Figure 3-81 presents the pre- and post-test pictures of the submerged carbon steel coupon. The surface of the coupon was roughened by the deposition of white precipitate. There were also areas of rust on the coupon.

Figure 3-79. CU-512 submerged, pre-test (left) and post-test (right).

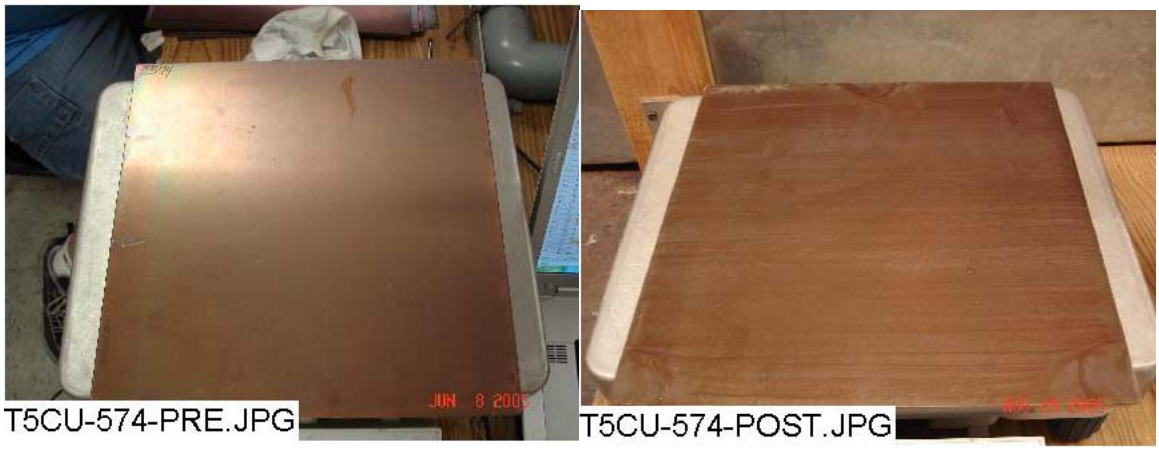

Figure 3-80. CU-574 submerged, pre-test (left) and post-test (right).

Figure 3-81. US-14 submerged, pre-test (left) and post-test (right).

Figure 3-82 presents the pre- and post-test pictures of the submerged concrete coupon. The post-test concrete coupon exhibits a brownish color.

Table 3-2 presents the pre- and post-test weight data for each representative submerged coupon.

The aluminum coupons' average weight differential was -11.2 g. The galvanized steel coupons' average weight gain was less than 0.1 g, and the coated steel coupons gained an average of 1.5 g. The representative copper coupons lost an average of 0.5 g, and the carbon steel coupon had no weight change. The concrete coupon gained 225.9 g, a gain of 3% of its original weight, which was likely due to post-test water retention.

Figure 3-82. Conc-003 submerged, pre-test (left) and post-test (right).

Table 3-2. Weight Data for Submerged Coupons

Type	Coupon No.	Pre-Test Wt. (g)	Post-Test Wt. (g)	Net Gain/Loss
Al	240	391.7	378.6	-13.1
Al	241	391.7	379.6	-12.1
Al	242	392.1	383.6	-8.5
GS	137	1043.2	1043.1	-0.1
GS	140	1067.5	1067.7	0.2
GS	141	1069.9	1070.0	0.1
IOZ	310	1652.9	1654.5	1.6
IOZ	312	1610.3	1611.6	1.3
CU	512	1322.6	1322.2	-0.4
CU	574	1306.0	1305.4	-0.6
US	14	1022.2	1022.2	0.0
Conc	003	7627.8	7853.7	225.9

3.4.1.2. Unsubmerged Coupons

Figures 3-83 and 3-84 show the pre- and post-test pictures of two unsubmerged aluminum coupons. Each unsubmerged aluminum coupon accumulated a white particle deposition along with some brownish areas. Also, the texture of each coupon is coarser, and the surface quality of each coupon is less lustrous than before the test. The reddish-brown color that was observed on the submerged coupons is absent on the unsubmerged coupons. The Al-247 coupon was loaded in Rack 2, which was located in the southern position of the middle tier of the tank. The Al-294 coupon was loaded in Rack 7, which was located in the northern position of the top tier of the tank.

Figure 3-83. Al-247 unsubmerged, pre-test (left) and post-test (right).

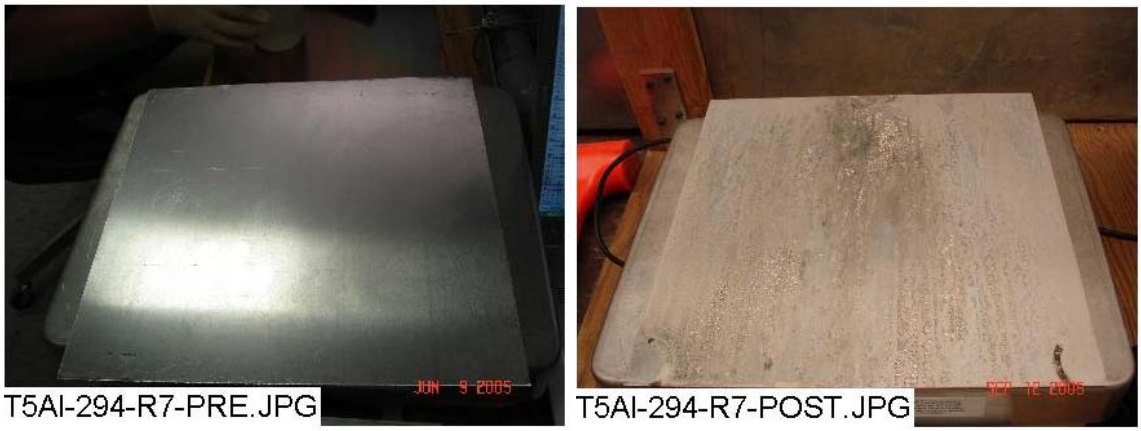

Figure 3-84. Al-294 unsubmerged, pre-test (left) and post-test (right).

Figures 3-85 and 3-86 show the pre- and post-test pictures of two unsubmerged galvanized steel coupons. There was some white deposition on the surface of these coupons, although it was in small amounts. This deposition is visibly different and less concentrated than that of the submerged coupons. The GS-167 coupon was loaded in Rack 3, which was located in the center position of the middle tier of the tank. The GS-638 coupon was loaded in Rack 6, which was located in the middle position of the top tier of the tank.

Figure 3-85. GS-167 unsubmerged, pre-test (left) and post-test (right).

Figure 3-86. GS-638 unsubmerged, pre-test (left) and post-test (right).

Figures 3-87 and 3-88 present the pre- and post-test pictures of two unsubmerged copper coupons. All of the copper coupons had vertical water marks that were likely caused by water flowing downward on the coupon surface during the spray portion of the test. The copper coupons did not appear to accumulate any particle deposition. The CU-430 coupon was loaded in Rack 2, which was located in the southern position of the middle tier of the tank. The CU-587 coupon was loaded in Rack 7, which was located in the northern position of the top tier of the tank.

Figure 3-87. CU-430 unsubmerged, pre-test (left) and post-test (right).

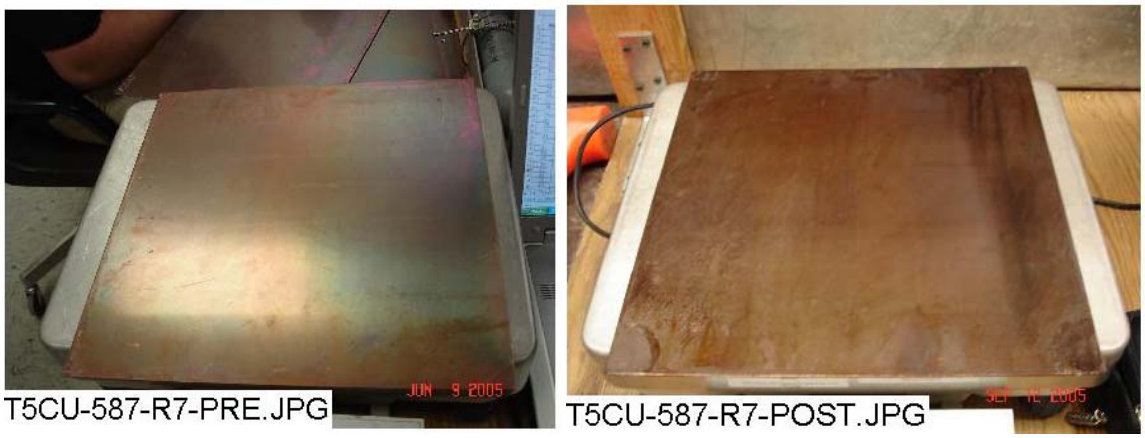

Figure 3-88. CU-587 unsubmerged, pre-test (left) and post-test (right).

Figures 3-89 and 3-90 present the pre- and post-test pictures of two unsubmerged IOZ-coated steel coupons. Each post-test coated steel coupon exhibits a similar pattern of deposition, which is less concentrated than that of the submerged coupons. The IOZ-342 coupon was loaded in Rack 4, which was located in the northern position of the middle tier of the tank. The IOZ-356 coupon was loaded in Rack 5, which was located in the southern position of the top tier of the tank.

Figure 3-89. IOZ-342 unsubmerged, pre-test (left) and post-test (right).

Figure 3-90. IOZ-356 unsubmerged, pre-test (left) and post-test (right).

Figure 3-91 presents the pre- and post-test pictures of one unsubmerged carbon steel coupon. The post-test carbon steel coupon exhibits rust along its center line and around its bottom edge. The deposition concentration is greater than that of the submerged carbon steel coupon. The US-18 coupon was loaded in Rack 6, which was located in the center position of the top tier of the tank.

Table 3-3 presents the pre- and post-test weight data for each representative unsubmerged coupon.

The aluminum coupons gained an average of 1.3 g, and the galvanized steel coupons lost an average of 0.2 g. The coated steel coupons' average weight gain was 1.6 g, and the copper coupons' average weight gain was 0.5 g. The carbon steel coupon lost 0.2 g.

Figure 3-91. US-18 unsubmerged, pre-test (left) and post-test (right).

Table 3-3. Weight Data for Unsubmerged Coupons

Type	Coupon No.	Pre-Test Wt. (g)	Post-Test Wt. (g)	Net Gain/Loss
Al	247	390.2	391.6	1.4
Al	294	390.6	391.8	1.2
GS	167	1051.6	1051.5	-0.1
GS	638	1067.5	1067.3	-0.2
IOZ	342	1656.0	1658.3	2.3
IOZ	356	1621.5	1622.5	1.0
CU	430	1319.8	1320.6	0.8
CU	587	1328.0	1328.2	0.2
US	18	1032.1	1032.3	0.2

Table 3-4 displays the mean weight gain/loss summary in grams for all of the submerged coupons. Table 3-5 displays the mean weight gain/loss summary in grams for all of the unsubmerged coupons by rack.

Table 3-4. Mean Gain/Loss Data for All Submerged Coupons (g)

Coupon Type	AL	GS	CU	IOZ	US	Concrete
Mean Gain - Loss (g)	-11.2	0.1	-0.2	1.6	0.0	225.9

Table 3-5. Mean Gain/Loss Data for All Unsubmerged Coupons (g)

	Mean Gain-Loss Per Coupon Type (g)				
Rack No.	AL	GS	CU	IOZ	US
2	0.8	0.6	0.4	1.4	n/a
3	0.1	<0.1	0.1	0.2	n/a
4	0.4	0.1	<0.1	1.1	0.2
5	0.9	<0.1	<0.1	1.1	n/a
6	0.4	0.1	0.1	1.5	0.2
7	1.2	0.3	0.2	1.8	n/a
Overall	0.4	0.2	0.2	1.2	0.2

3.4.2. SEM Analyses of Coupons

3.4.2.1. Submerged Coupons

During the ICET tests, trace metal cations may be released from the submerged metal coupon surfaces due to corrosion effects. Subsequently, the released metal cations may form complexes in solution through electrostatic interactions with anions such as OH^-,

$B_4O_7^{2-}$, $H_2BO_3^-$, SiO_3^{2-}, and CO_3^{2-}. In addition, the complexed anions may attract other cations from the solution, such as Ca^{2+}, Mg^{2+}, Al^{3+}, Cu^{2+}, Zn^{2+}, and H^+. As a result, corrosion products (deposits) are formed and may continuously grow on the metal coupon surfaces. The thickness of the deposits was observed to be in the range of millimeters. The adherence between the metal coupons and the deposits is through chemical bonds, which are much stronger than van der Waals forces. Due to the vertical orientation of the metal coupons in the tank (with a small horizontal cross-sectional area), the deposits on the metal coupon surface are likely of chemical origin, rather than being the result of particulate deposits settling on the surface.

According to the SEM/EDS results, the dominant corrosion products on the submerged Al coupons are likely aluminum hydroxide with other substances containing Si, Ca, O, C, Fe, and Cu. For submerged Cu coupons, the possible corrosion products include CuO, $Cu_2(CO_3)(OH)_2$, and substances containing Cu, Ca, Si, Al, O, and C. For the submerged galvanized steel coupons, the possible corrosion products are oxides, hydroxides, silicate, and carbonate compounds of Zn, Ca, and Al. For the submerged steel coupon, the possible corrosion products include oxide, hydroxide, silicate, and carbonate compounds of Fe and Ca and compounds composed of Fe, Si, Ca, O, and Al.

3.4.2.2. Unsubmerged Coupons

The physical and chemical changes that the unsubmerged coupons experienced during Test #5 are less significant than the changes experienced by the submerged coupons. The unsubmerged coupons were affected by the test solution only during the initial 4-hour spray phase. They were also exposed to moisture vapor throughout the test.

According to SEM/EDS results, the dominant corrosion products on the unsubmerged Al coupons are likely aluminum hydroxide and/or aluminum oxide. For unsubmerged Cu, the corrosion products on the coupon surface are likely CuO; $Cu_2(CO_3)(OH)_2$; and the corrosion products containing Al, Si, O, Ca, Cu, Na, Fe, and C. The corrosion products on the unsubmerged galvanized steel coupon surface are composed of C, O, and Zn. They are likely ZnO and $ZnCO_3$. For the unsubmerged steel coupon, the likely corrosion products are Fe_2O_3, $Fe(OH)_3$, $Fe_2(CO_3)_3$, and compounds containing small amounts of Si.

The complete listing of Day-30 coupon analysis is shown in Appendix E.

3.5. Sedimentation

Sediment was collected from the tank bottom after the test solution was drained. The entire amount recovered was 89 g, wet, as shown in Figure 3-92. Figure 3-93 shows the tank bottom with the sediment, after the test solution was drained and the samples were removed. Figure 3-94 shows the top of the drain screen with the drain collar still attached.

Figures 3-95 through 3-99 and Table 3-6 provide SEM/EDS and XRD/XRF analysis results. The SEM/EDS and XRD/XRF analyses provided information on the morphology and composition of Test #5 sediment. SEM images show that the sediments were mainly

composed of fiberglass debris, which mixed with some particulate deposits. Consistently, the XRF result shows that SiO_2 was about 64% of the total mass of the dried sediments. In addition, the XRD result indicates the presence of quartz crystal in the sediments. The quartz is likely from a crystalline form of fiberglass debris. The particulate deposits in the sediments possibly originated from the corrosion products, chemical precipitates, concrete debris, and dust.

It should be noted that the XRD result also shows the possible crystalline match of cobalt and uranium compounds in the sediments. However, cobalt and uranium were unlikely present in the testing material. Their match patterns are likely due to the variety of species contained within the sediment. As a result, these compounds may be excluded from the sediment compositions.

The complete Day-30 sediment analyses are given in Appendix F.

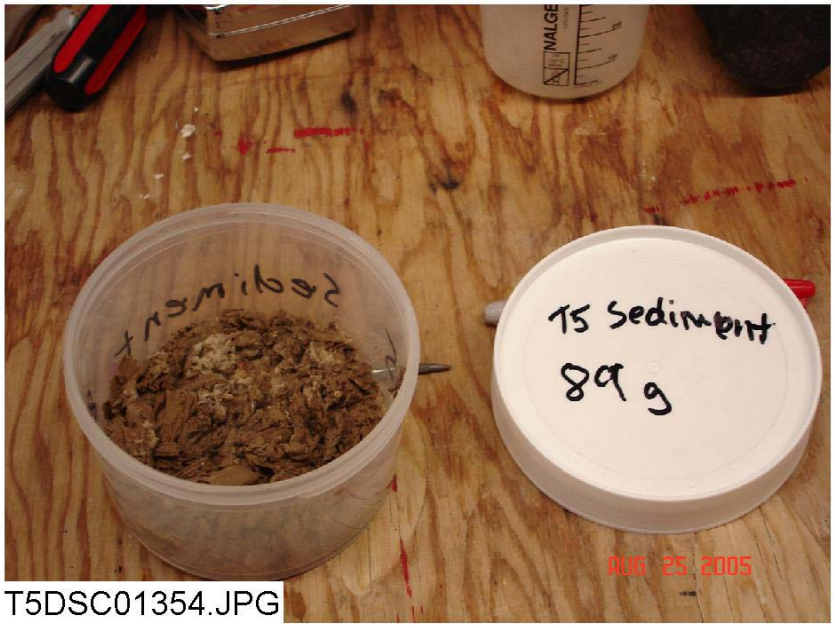

Figure 3-92. Sediment removed from the tank.

Figure 3-93. Tank bottom after draining.

Figure 3-94. Drain collar removed from the tank bottom.

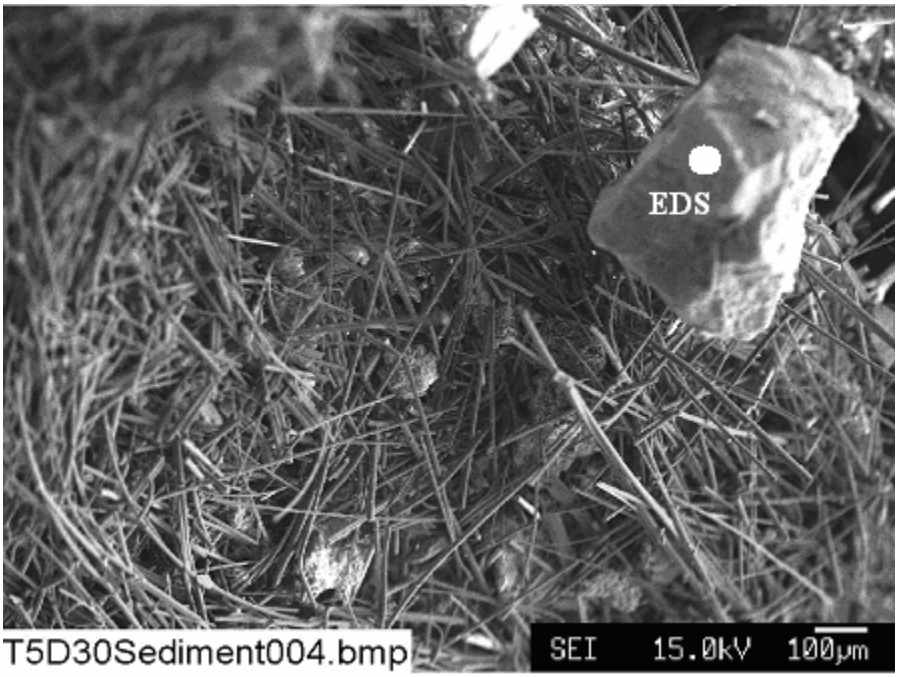

Figure 3-95. SEM image magnified 70 times for the Test #5, Day-30 sediment at the bottom of the tank.

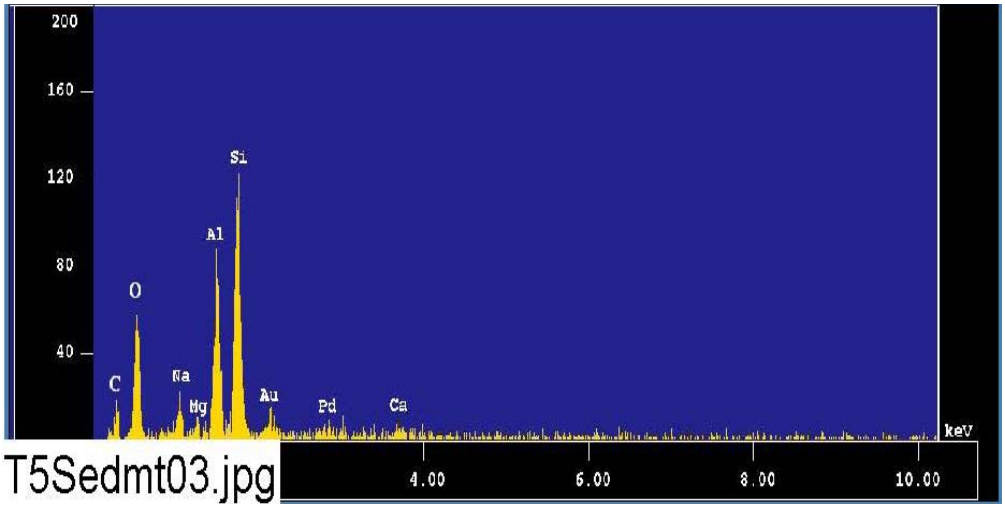

Figure 3-96. EDS counting spectrum for the big particulate deposit shown in Figure 3-95.

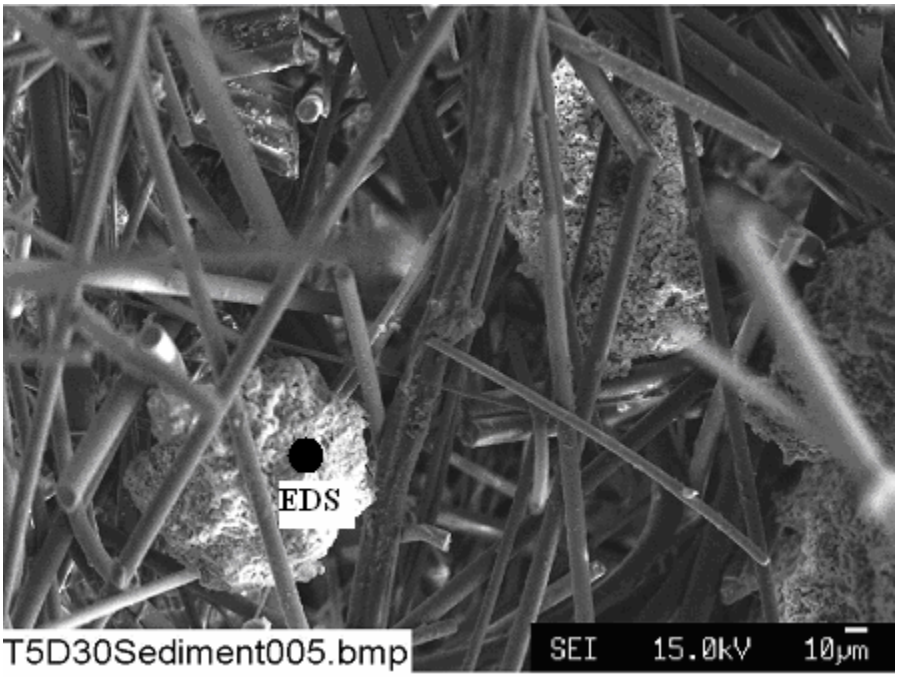

Figure 3-97. SEM image magnified 300 times for the Test #5, Day-30 sediment at the bottom of the tank.

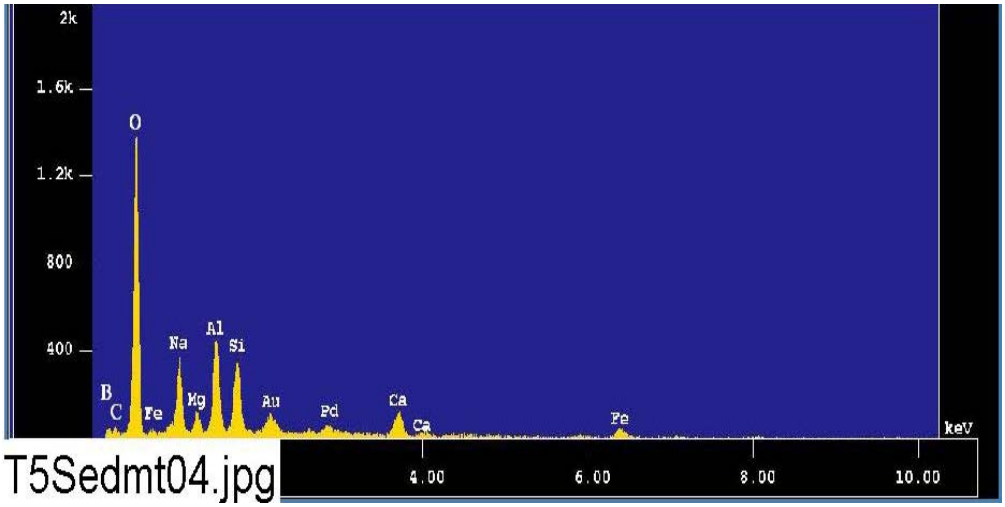

Figure 3-98. EDS counting spectrum for the particulate deposit shown in Figure 3-97.

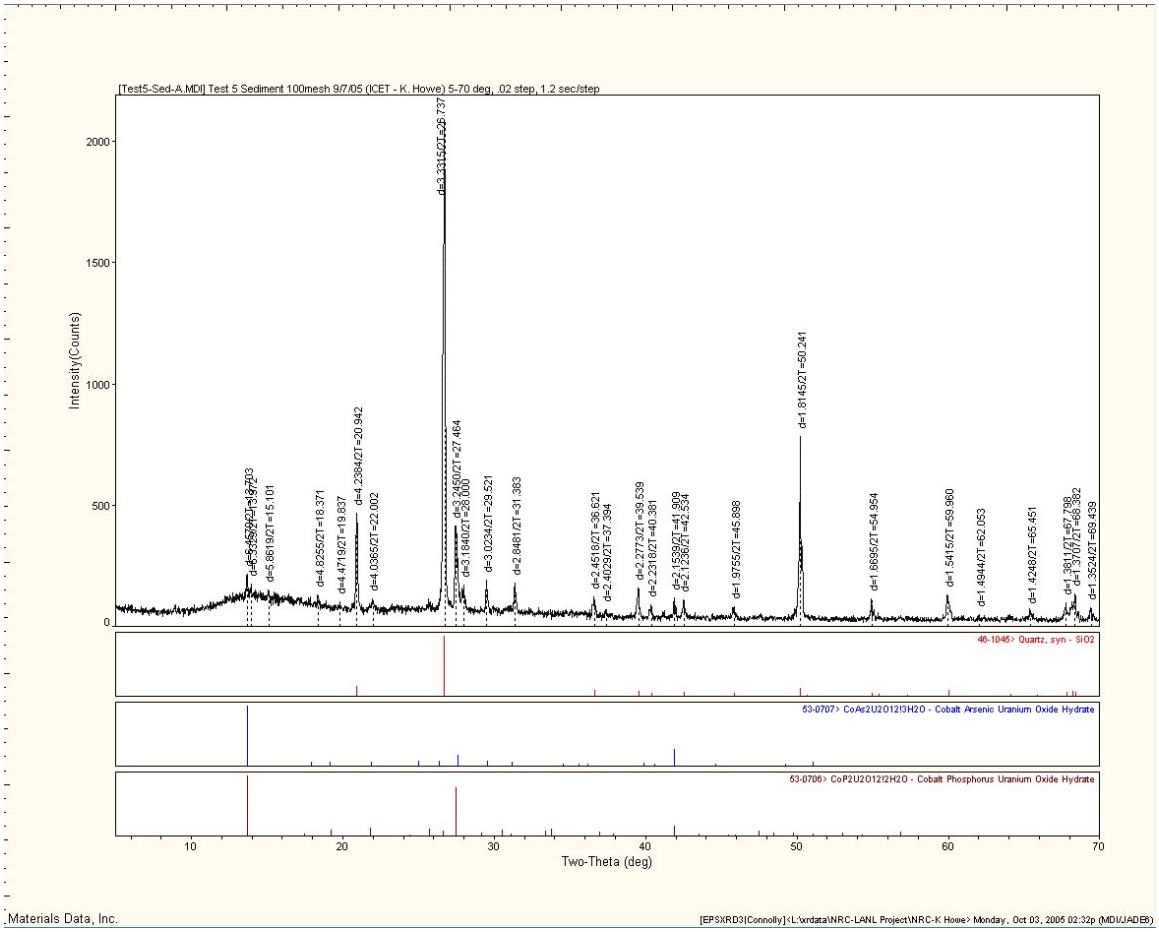

Figure 3-99. XRD result of the possible matching crystalline substances in Test #5, Day-30 sediment.

Table 3-6. Dry Mass Composition of Test #5, Day-30 Sediment by XRF Analysis

First row is chemical component; second row is mass composition (%).

SiO_2	TiO_2	Al_2O_3	Fe_2O_3	FeO	MnO	MgO	CaO	Na_2O	K_2O	$H_20(-)$	$H_2O(+)CO_2$	P_2O_5	Total
63.76	0.18	6.00	1.34	0.00	0.07	1.78	5.49	9.28	1.09	0.69	3.27	0.07	93.02

3.6. Deposition Products

For the ICET tests, one concern is the deposition of debris/corrosion products in the tank. To help understand this problem, the corrosion/deposition products were collected after completion of the test. These products are fine yellow powders removed from the submerged CPVC rack. SEM/ EDS results shown in Figures 3-100 through 3-102 indicate that the fine yellow powders were mainly composed of fiberglass debris and particulate deposits containing O, Na, Al, C, Ca, Mg, and possibly Si.

Figure 3-100. SEM image magnified 200 times for the Test #5, Day-30 fine yellow powder on the submerged rack.

Figure 3-101. Annotated SEM image magnified 1000 times for the Test #5, Day-30 fine yellow powder on the submerged rack.

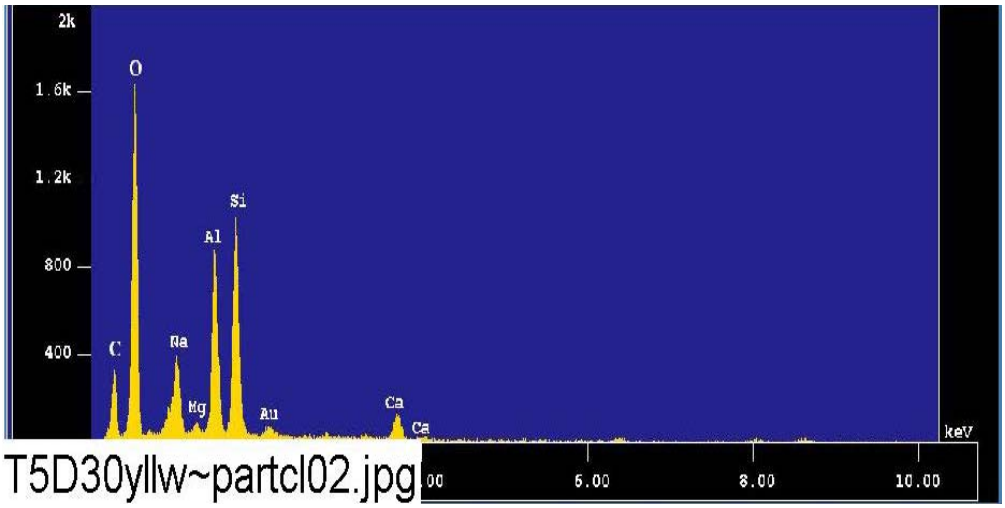

Figure 3-102. EDS counting spectrum for the particulate deposit shown in Figure 3-101.

3.7. Optical/TEM Images

The TEM images and EDS results for Test #5, Day-4, Day-15, and Day-30 unfiltered solution samples are shown in Appendix G. The unfiltered solution samples were extracted from the tank directly. A tiny drop of the test solution was transferred to a copper mesh and dried in air for TEM analysis.

TEM results show the presence of submicron-size colloidal particles in the samples (see Figures 3-103 through 3-105). However, it is unclear if the colloidal particles originally existed in the test solution or were formed during the drying process before TEM examination.

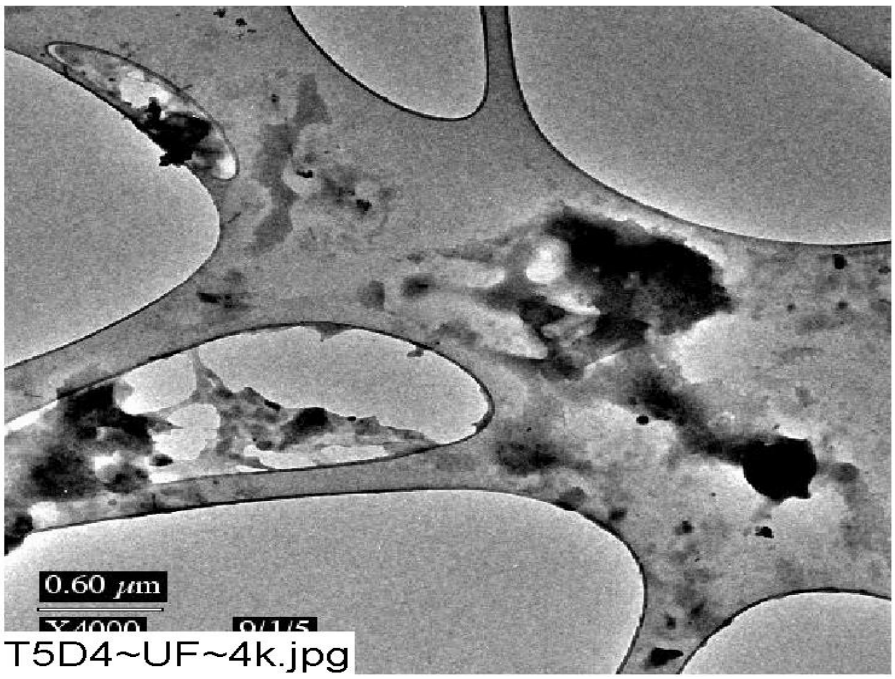

Figure 3-103. TEM magnified 4000 times for one Test #5, Day-4 unfiltered sample location.

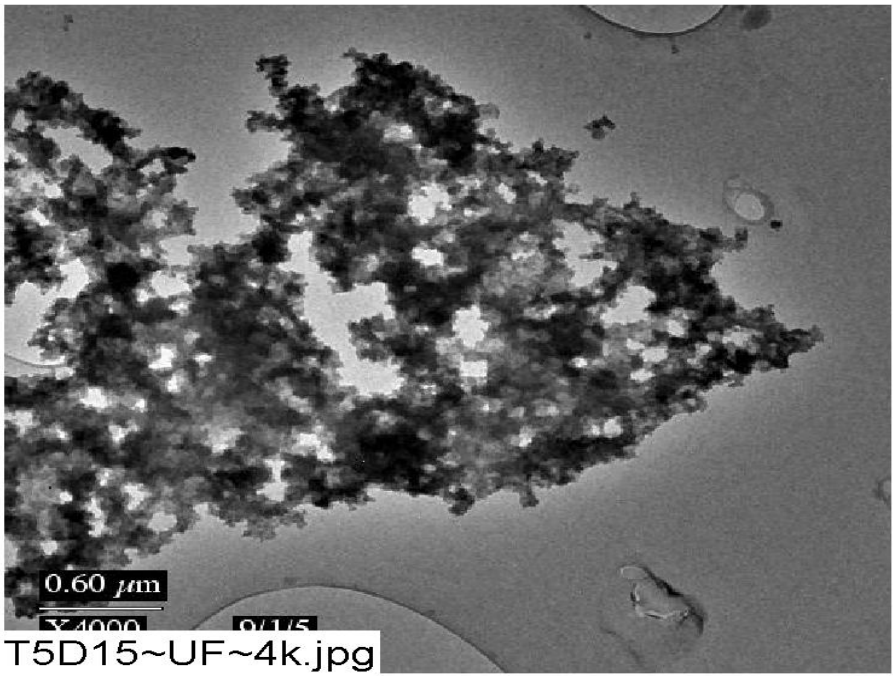

Figure 3-104. TEM magnified 4000 times for one Test #5, Day-15 unfiltered sample location.

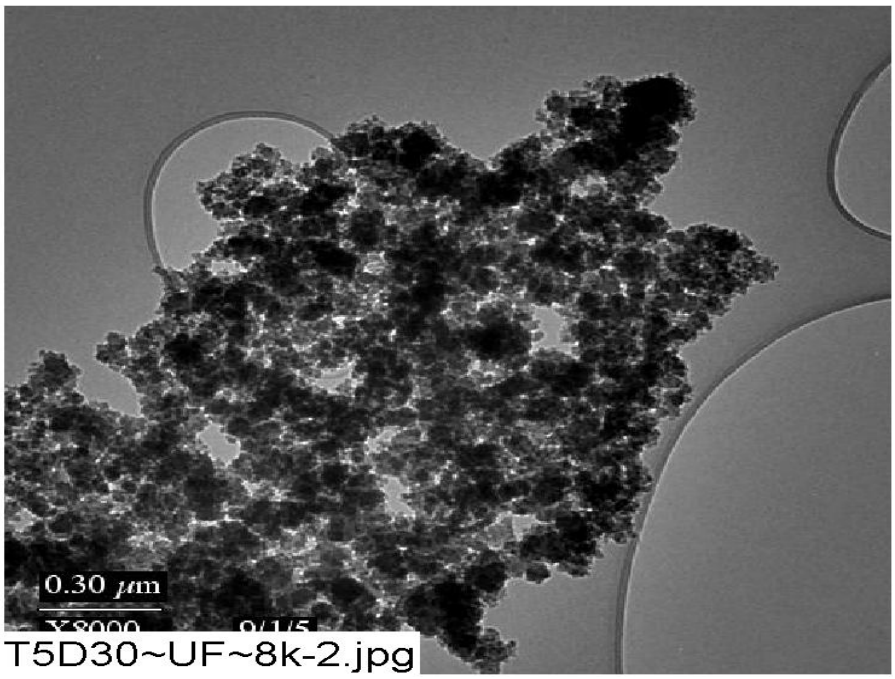

Figure 3-105. TEM magnified 8000 times for one Test #5, Day-30 unfiltered sample location.

3.8. UV Absorbance Spectrum

UV absorbance was measured for the Day-30 filtered solution sample and is shown in Appendix H. The purpose of this analysis was to identify the presence of any distinguished absorbance peaks that may identify organics present in the solution. However, based on the result, no distinguished absorbance peaks were found due to the heterogeneous nature of the test solution.

3.9. Shear-Dependent Viscosity

As explained in the Test #1 data report (Ref. 2), shear-rate viscosity measurements were taken weekly on test solution samples. The Test #1 solution at 25ºC exhibited shear-thinning behavior, indicative of a non-Newtonian fluid. The solutions for Tests #2, #3, and #4 were all Newtonian fluids at 25ºC.

As with Test #1, the Test #5 solution at 25ºC exhibited shear-thinning behavior, as shown in Figure 3-106. The legend for the symbols gives the date the samples were remove from the solution. For example, “072705” is Day 2, and “082505” is Day 30. Shear thinning is indicated by the decrease in viscosity as the shear rate is increased to 20 1/s. Additionally, the solution’s viscosity increases at all shear rates with time over the test duration, with one exception. The last sample taken on Day 30 (082505-0900-U) decreased to a value similar to that of the mid-test sample. While there is no definitive explanation for the decrease, it may be related to the late-test behavior of the turbidity, TSS, and aluminum and calcium concentrations.

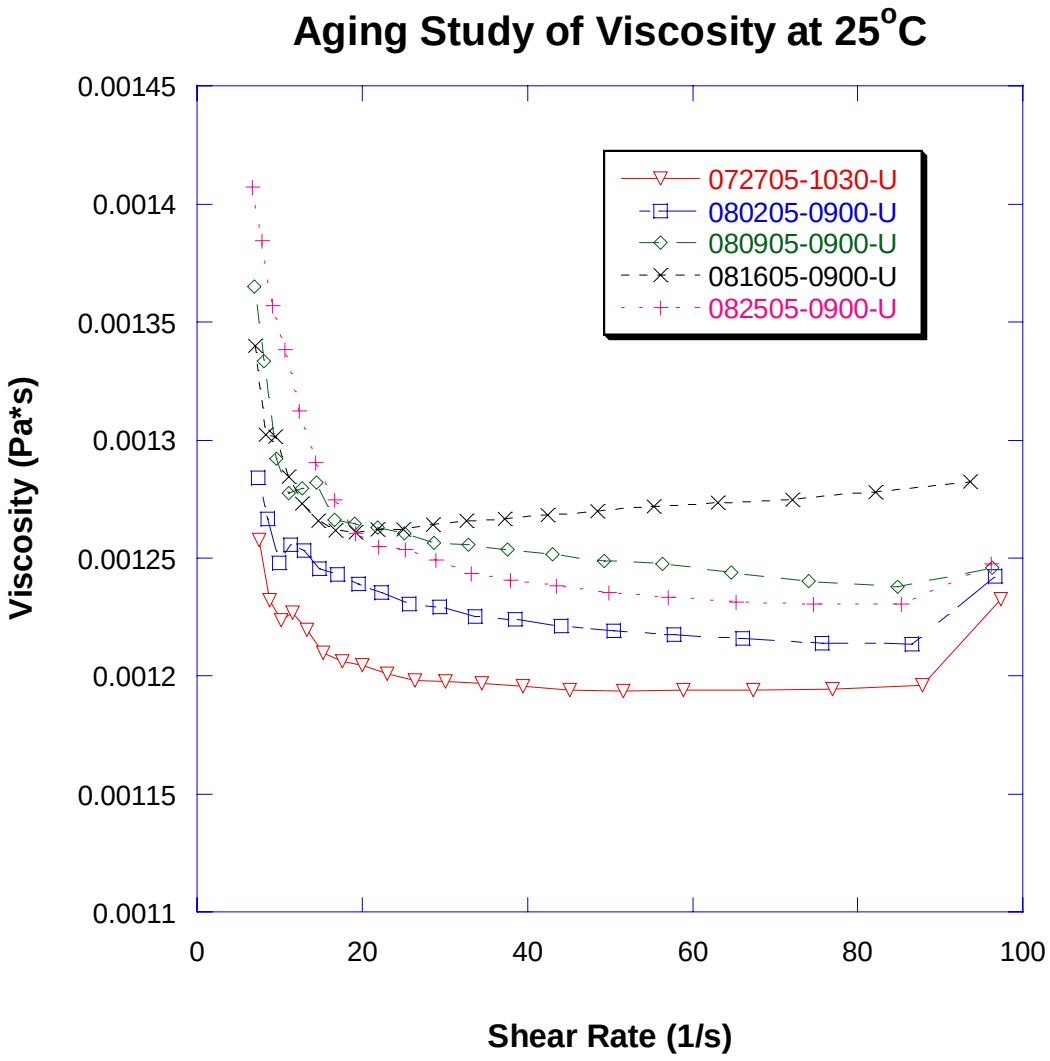

Figure 3-106. Shear-rate viscosity measurements at 25ºC.

This page intentionally left blank.

4. SUMMARY OF KEY OBSERVATIONS

ICET Test #5 ran for 30 days, and all conditions were maintained within the accepted flow and temperature ranges, with one exception. On Day 5, the addition of cold makeup water caused the test solution temperature to drop to 57.7ºC, which is 0.3ºC below the target minimum. The minimum temperature was below 58.0ºC for less than 10 minutes. At the start of the test, the measured pH was 8.4. During the addition of hydrochloric acid, the pH dropped slightly to 8.3, and it remained between 8.2 and 8.4 for the duration of the test. The test solution turbidity decreased to approximately 2 NTU after 7 days. The turbidity at 60ºC decreased to approximately 1 NTU the following day and remained near 1 NTU for the duration of the test. However, when the solution was cooled to 23ºC, the turbidity increased to 5 NTU at Day 19 and remained near that value for the duration of the test.

Samples of the solution were taken daily. Analyses of the test solution showed that aluminum in the solution rose above 50 mg/L on Day 11 and fluctuated between 33 and 55 mg/L for the duration of the test. Calcium, silica, sodium, chloride, and boron were also prevalent in the solution.

Daily measurements of the constant-shear kinematic viscosity of the test solution revealed an approximately constant value at both test temperature and room temperature. Measurements of the shear-dependent viscosity indicated that at 60°C the test solution remained Newtonian for the entire test. At 25°C, the test solution exhibited shear-thinning behavior, and the viscosity generally increased at all shear rates as the test progressed. Light, wispy precipitates were visible after the test solution sat at room temperature for several days.

Examinations of fiberglass taken from the test apparatus revealed chemical byproducts and web-like deposits that spanned individual fibers. Flocculent deposits were also observed. The amounts of these deposits did not appear to increase significantly over the duration of the test, and the web-like deposits were absent in the Day-30 samples. The deposits were likely formed by chemical precipitation. In addition to these deposits, some samples had significant amounts of particulate deposits on their exteriors that were likely physically attached.

The submerged metallic coupons all developed thin particulate deposits that dulled their color and roughened their surface. Post-test examinations showed that the submerged aluminum coupons lost approximately 3% of their weight, but there were very little weight changes on the other coupons. The unsubmerged coupons exhibited some streaking but little or no weight change.

After the tank was drained, there was very little sediment on the tank bottom, but powdery deposition products were present on the submerged objects.

REFERENCES

1. "Test Plan: Characterization of Chemical and Corrosion Effects Potentially Occurring Inside a PWR Containment Following a LOCA, Rev. 13," July 20, 2005.

2. J. Dallman, J. Garcia, M. Klasky, B. Letellier, and K. Howe, "Integrated Chemical Effects Test Project: Test #1 Data Report," LA-UR-05-0124, June 2005.

3. "Pre-Test Operations, Test #5," ICET-PI-017, Rev. 0, July 22, 2005.

4. "Test Operations, Test #5 (fiberglass and sodium tetraborate at pH 8)," ICET-PI-018, Rev. 0, July 22, 2005.

5. "Post-Test Operations, Test #3," ICET-PI-008, Rev. 3, May 2, 2005.